Fluorescence of Rb in a sub-micron vapor cell: spectral resolution of atomic transitions between Zeeman sublevels in moderate magnetic field

D. Sarkisyan, A. Papoyan, T. Varzhapetyan

Institute for Physical Research, Armenian National Academy of Sciences, Ashtarak-2, 378410, Armenia

K. Blushs, M. Auzinsh

Department of Physics, University of Latvia, 19 Rainis boulevard, Riga, LV-1586, Latvia

It is experimentally demonstrated that the use of an extremely thin cell (ETC) with the thickness of Rb atomic vapor column of ~ 400 nm allows one to resolve a large number of individual transitions between Zeeman sublevels of D_1 line of ^{87}Rb and ^{85}Rb in the sub-Doppler fluorescence excitation spectra in an external magnetic field of ~ 200 G. It is revealed that due to the peculiarities of Zeeman effect for different hyperfine levels of Rb all allowed transitions between magnetic sublevels can be clearly resolved for ^{87}Rb $F_g = 1 \rightarrow F_e = 1, 2$ and $F_g = 2 \rightarrow F_e = 1, 2$ fluorescence excitation. Also, relatively good spectral resolution can be achieved for ^{85}Rb $F_g = 2 \rightarrow F_e = 2, 3$ fluorescence excitation. Some partial resolution of transitions between magnetic sublevels is achieved for ^{85}Rb $F_g = 3 \rightarrow F_e = 2, 3$ fluorescence excitation. The spectral resolution of individual transitions allows one to easily observe both linear and nonlinear Zeeman effects in the fluorescence excitation spectra obtained with the help of the ETC. In the fluorescence spectra of a cell of

usual length there is no evidence of a spectral resolution of individual transitions at $B \sim 200$ G. A simple magnetometer based on ETC with Rb with a sub-micron spatial resolution is described.

PACS numbers: 32.60.+i, 32.10.Fn, 32.70.Jz

I. INTRODUCTION

Experimental realization of sub-Doppler spectroscopy of atomic vapors based on a thin cell with a column length $L \sim 10 - 1000$ μm has been reported in [1, 2]. However, revealing a sub-Doppler structure in transmission spectrum in this case requires a frequency modulation (FM) technique to be implemented for enhancement of the contrast of narrow resonances [1, 2]. Meanwhile a simple laser-diode technique is sufficient to resolve spectrally atomic hyperfine transitions in alkali atoms thanks to the usage of the extremely thin cells (ETC) with $L \sim 100 - 600$ nm [3, 4]. The sub-Doppler profile of the hyperfine transition in the case of the fluorescence excitation spectra in ETC is narrower than that of transmission and hence, for some applications it is more convenient to use the fluorescence excitation spectrum [3, 4].

Very recently it was demonstrated that the laser spectroscopy based on ETC is a convenient tool to investigate behavior of transitions between individual hyperfine states of Cs and Rb D_2 lines in a magnetic field of moderate strength. In these experiments a magnetic field induced strong circular dichroism was observed [5, 6]. However, due to the large number of magnetic sublevels and as a result of many allowed transitions between individual pairs of magnetic sublevels for a hyperfine transitions of Cs and Rb D_2 lines it was impossible to spectrally resolve these transitions at a moderate strength of a magnetic field.

The aim of the present work was an experimental demonstration of a possibility of complete resolution of the transitions between Zeeman sublevels in the fluorescence excitation spectrum and clarification of possible applications. To reach this aim a resonant D_1 transition in Rb was excited in ETC placed in a moderate strength magnetic field. Although saturation absorption (SA) spectroscopy provides narrower spectral lines, the advantage of the spectroscopy in ETC is the absence of crossover resonances with large amplitudes. Moreover, substantial nonlinearity of the atomic response in SA and its strong dependence on the external conditions may strongly modify the spectrum in a magnetic field.

II. EXPERIMENTAL: APPARATUS AND RESULTS

The experimental setup is presented in Fig.1*a*. The beam (Ø 3 mm) of the wavelength $\lambda = 794$ nm, and line-width 25 MHz from a single-frequency *cw* laser diode was directed at a normal incidence onto the ETC. The design of the ETC (which has garnet windows) is similar to the one presented earlier [3, 4]. As it was shown [7, 8], the most narrow sub-Doppler line-width of the hyperfine transition is achieved, when vapor column length $L = \lambda/2$. That was the reason why the thickness of atomic vapor column of Rb was chosen to be $L = \lambda/2 \sim 400$ nm. The column thickness L has been measured by the interferometric technique presented earlier [7]. The ETC operated with a specially designed oven with 4 openings: 2 openings for the laser beam transmission, and 2 openings (orthogonal to the previous pair) for the side fluorescence detection. This geometry allows one to simultaneously detect fluorescence and transmission spectra. The fluorescence was detected by a photodiode with an aperture of ~ 1 cm^2, which was placed at a 90° angle to the laser radiation propagation direction. The signal of the photodiode was recorded by a two-channel digital storage oscilloscope. The temperature T_{sa} of the side-arm of the ETC was kept at ~ 120

°C (to prevent metal vapor condensation the temperature of windows was kept $\sim$ 10 °C higher). Side-arm temperature provides vapor density of ^{85}Rb and ^{87}Rb $N \sim 6 \times 10^{12}$ cm^{-3} and 1.5×10^{13} cm^{-3} correspondingly.

The ETC was placed in the center of 3 pairs of mutually orthogonal Helmholtz coils providing possibility to apply a homogeneous magnetic field in an arbitrary direction. A Glan prism was used to purify the linear polarization of the laser diode radiation; to produce a circular polarization, an antireflection coated quarter wave plate was utilized. Geometrical configuration of the measurements is shown in Fig.1*b*.

Additional beam splitter directed 50% of the laser beam to the second ETC filled with Rb. The fluorescence signal from the second ETC has been used as a frequency and amplitude reference for $B = 0$ (light curves in the figures 2 – 4).

It has been demonstrated that the line-width of the fluorescence excitation spectrum in an ETC on the individual hyperfine transition could be $\sim$ 10 times narrower than the Doppler linewidth [3, 4], and thus all the hyperfine transitions of Rb D_1 line are resolved in the absence of the magnetic field ($B = 0$).

The fluorescence excitation spectra of ^{87}Rb in a longitudinal magnetic field $B = 225$ G ($\mathbf{B} \parallel \mathbf{k}$) with σ^+ excitation is presented in Fig.2*a*. It is easy to identify five peaks that correspond to the following $F_g = 1 \rightarrow F_e = 1, 2$ components, in order of frequency increase, see Fig.2*a*, lower part: $F_g = 1$, $m_F = -1, 0 \rightarrow F_e = 1$, $m_F = 0, +1$ respectively, and $F_g = 1$, $m_F = -1, 0, +1 \rightarrow F_e = 2$, $m_F = 0, +1, +2$, respectively. The fluorescence spectra of ^{87}Rb $F_g = 2 \rightarrow F_e = 1, 2$ in the case of longitudinal magnetic field $B = 225$ G ($\mathbf{B} \parallel \mathbf{k}$) with σ^- excitation is presented in Fig.2*b*. It is also easy to identify seven peaks that correspond to the atomic transitions presented in the diagram of Fig.2*b*, lower part (for ^{87}Rb spectra excited in other configurations, see [9]). Indicated values of the level shifts are given under

assumption of a linear Zeeman effect regime. This is for reference purposes only. It is not strictly valid for a magnetic fields' strength used in this experiment.

The fluorescence spectra in the case of longitudinal magnetic field $B = 225$ G ($\mathbf{B} \parallel \mathbf{k}$) with σ^+ and σ^- excitations for ^{85}Rb $F_g = 2 \rightarrow F_e = 2, 3$ are presented in Fig.3*a,b*. For transversal magnetic field ($\mathbf{B} \parallel \mathbf{E}$) with π (linear) excitation, the fluorescence spectrum is presented in Fig.3*c*. As it is seen, for σ^+ excitation there is a relatively good spectral resolution of each individual transition between Zeeman sublevels (9 resolved transitions). Relevant transitions between Zeeman sublevels are presented in Fig.3, lower part.

The 9 resolved peaks in the Fig.3*a* correspond, in order of frequency increase, to the transitions $F_g = 2$, $m_F = -2, -1, 0, +1 \rightarrow F_e = 2$, $m_F = -1, 0, +1, +2$ (4 peaks) respectively, and $F_g = 2$, $m_F = -2, -1, 0, +1, +2 \rightarrow F_e = 3$, $m_F = -1, 0, +1, +2, +3$ (5 peaks) respectively. In the case of σ^- excitation and π (linear) excitation, the fluorescence spectra for $B = 225$ G presented in Fig.3*b,c* demonstrate a partial overlapping of the transitions.

The fluorescence spectra in the case of longitudinal magnetic field $B = 225$ G ($\mathbf{B} \parallel \mathbf{k}$) with σ^+ and σ^- excitations for ^{85}Rb $F_g = 3 \rightarrow F_e = 2, 3$ and for transversal magnetic field ($\mathbf{B} \parallel \mathbf{E}$) with π (linear) excitation are presented in Fig.4*a,b,c*. Relevant transitions between the Zeeman sublevels are presented in the Fig.4, lower part.

III. LASER-INDUCED-FLUORESCENCE EXCITATION SPECTRA IN A MAGNETIC FIELD. SIGNAL SIMULATION.

To simulate laser-induced-fluorescence excitation (LIFE) spectra of Rb atoms in a magnetic field of intermediate strength we will use the following model. We will assume that laser radiation is weak and absorption rate is small in comparison with the relaxation rates in ground and excited states. This assumption is well justified by the observation of LIFE

spectrum independence from the laser intensity.

The Hamilton operator of the atom in a magnetic field can be written as

$$\widehat{H} = \widehat{H}_0 + \widehat{H}_{HFS} - \mu_J \cdot \mathbf{B} - \mu_I \cdot \mathbf{B}. \tag{1}$$

where $\widehat{H}_0$ is a Hamiltonian operator of unperturbed atom without taking into account nuclei spin, $\widehat{H}_{HFS}$ represents hyperfine interaction. The remaining two terms represent interaction of the electronic magnetic moment μ_J of atom and the nucleus magnetic moment μ_I with the external magnetic field $\mathbf{B}$. These magnetic moments are related to the respective electronic and spin angular moments $\mathbf{J}$ and $\mathbf{I}$ of the atom

$$\mu_J = \frac{g_J \mu_B}{\hbar}\mathbf{J}, \qquad \mu_I = \frac{g_I \mu_0}{\hbar}\mathbf{I}, \tag{2}$$

where μ_B and μ_0 are the Bohr and nuclear magnetons respectively and g_J; g_I are electrotonic and nuclear Landé factors. The action of a magnetic field on the atom has two closely related effects. Firstly, in the magnetic field magnetic sublevels of the hyperfine levels are mixed by this field, giving rise to new atomic states, which are a linear combination of initial hyperfine levels:

$$|\gamma_k m\rangle = \sum_{F_e=|J_e-I|}^{F_e=J_e+I} C^{(e)}_{kF_e}(B,m)\,|F_e,m\rangle\,, \tag{3}$$

$$|\eta_j \mu\rangle = \sum_{F_g=|J_g-I|}^{F_g=J_g+I} C^{(g)}_{jF_g}(B,\mu)\,|F_g,\mu\rangle\,, \tag{4}$$

where $C^{(e)}_{kF_e}(B,m)$ and $C^{(g)}_{jF_g}(B,\mu)$ are mixing coefficients depending on the field strength and magnetic quantum number m and μ of the excited and ground state. The second effect is a deviation of the Zeeman magnetic sublevel splitting in the magnetic field for each hyperfine level from the linear one. It means that the additional energy of the magnetic sublevel obtained in the magnetic field is not any more linearly proportional to the field

strength. For D_1 transition four new atomic states $|\gamma_k m\rangle$ and $|\eta_j \mu\rangle$ are formed in the magnetic field for each isotope (2 in case of Rb atoms in the $5P_{1/2}$ state and 2 in case of Rb atom in the $5S_{1/2}$ state). As it is seen from Eq. (4), in the magnetic field hyperfine angular momentum quantum number F ceases to be a good quantum number, but magnetic quantum numbers m and μ are still good quantum numbers. This reflects the symmetry of the perturbation imposed by the magnetic field and means that only hyperfine sublevels with the same magnetic quantum numbers are mixed by the magnetic field.

The mixing coefficients $C^{(e)}_{kF_e}(B,m)$ and $C^{(g)}_{jF_g}(B,\mu)$ of the hyperfine states in the magnetic field and energies of these levels in the field ${}^{\gamma_k}E_m$, ${}^{\eta_j}E_\mu$ can be found as eigenvectors and eigenvalues of the Hamilton matrix (1). In case of two hyperfine levels this problem has an analytical solution known as Breit – Rabi formula, see, for example [10].

The conditions of the experiment – diode laser excitation in a stationary regime – allow us to use a relatively simple theoretical model for LIFE spectrum simulation – namely, so-called *rate equations* for Zeeman coherences, see [11–13] and recent analysis of a relation of rate equations to optical Bloch equations for density matrix [14]. As it is shown in [14], in present conditions both approaches are equivalent. The configuration of the cell and linear excitation regime (laser intensity below saturation) allow us to a good approximation consider just one velocity group of atoms moving perpendicularly to the laser beam and neglect the effects of optical pumping, transition saturation and reabsorption. The one-velocity-group approximation also means that we can consider near-resonant excitation of atoms – and this allows us to assume the laser line-shape as Lorentzian. Lorentzian is a good approximation of the center of the laser line. Considering the above assumptions, rate equations take the following form [14]:

$$\frac{\partial\, {}^{kl} f_{m_i m_j}}{\partial t} = -i\omega_{m_i m_j} f_{m_i m_j} - \Gamma f_{m_i m_j} + \\ + \Gamma_p \sum_{\mu} \langle \gamma_k m_i | \, \mathbf{d}\cdot\mathbf{e} \, | \eta\mu \rangle \, \langle \eta\mu | \, \mathbf{d}\cdot\mathbf{e}^* \, | \gamma_l m_j \rangle = 0 \tag{5}$$

$$\Gamma_p = \frac{|\varepsilon_{\overline{\omega}}|^2}{\hbar^2} \frac{(\Gamma + \triangle\omega) + i\left(\omega_{m_i\mu} + \omega_{\mu m_j}\right)}{\left[\left(\frac{\Gamma}{2} + \frac{\triangle\omega}{2}\right) + i\left(\overline{\omega} + \omega_{\mu m_j}\right)\right] \times \left[\left(\frac{\Gamma}{2} + \frac{\triangle\omega}{2}\right) - i\left(\overline{\omega} - \omega_{m_i\mu}\right)\right]} \tag{6}$$

$f_{m_i m_j}$ is an excited state density matrix, ω_{ij} denotes the Zeeman splitting ($\omega_{ij} = \dfrac{E_i - E_j}{\hbar}$), Γ is the total excited state relaxation rate, $|\varepsilon_{\overline{\omega}}|$ is the amplitude of the electric field of definite polarization $\mathbf{e}$, $\triangle\omega$ is the laser line-width (FMHM), $\overline{\omega}$ is the central frequency of the laser spectrum. The transition dipole matrix elements of the type $\langle i | \, \mathbf{d}\cdot\mathbf{e} \, | j \rangle$ can be calculated using the standard angular momentum algebra [15–17].

At each laser frequency a specific density matrix is calculated. Generally, the intensity of the fluorescence with a specific polarization $\mathbf{e}_{obs}$ in a transition between excited γ_k and final η_j state in the magnetic field can be calculated according to:

$$I\left(\mathbf{e}_{obs}\right) = I_0 \sum_{mm'\mu} \sum_{klj} \langle \gamma_k m | \, \mathbf{e}^*_{obs}\cdot\mathbf{d} \, | \eta_j \mu \rangle \, \langle \gamma_l m' | \, \mathbf{e}^*_{obs}\cdot\mathbf{d} \, | \eta_j \mu \rangle \; {}^{kl} f_{mm'}, \tag{7}$$

see for example [15]. In this particular experiment, to have LIFE spectrum we assume that in the specific direction of observation light with all polarization is detected (no analyzer in a detection system) and all possible transitions in fluorescence are observed (no spectral selection in detection system). For this, Eq. (7) is averaged over all polarizations and final states of the transition.

This approach to spectrum calculation in the magnetic field and in absence of the field was used in the following simulation of experimentally observed signals.

IV. DISCUSSION

Application of a magnetic field causes different energy shifts for different Zeeman sublevels, lifting the degeneracy, and pure non-degenerate atomic transitions can be recorded. A simple analysis shows that the following conditions are favorable for this purpose: opposite signs of Landé factors g_F of the ground and the excited levels, so that the transition frequency shift is enhanced, with g_F values as large as possible; a small value of F for the ground and the excited states in order to have less magnetic sublevels. Taking into account these conditions, the most convenient transition system is ^{87}Rb D_1 $F_g = 1, 2 \rightarrow F_e = 1, 2$. In fact, atomic transitions between the individual Zeeman sublevels in the ETC on ^{87}Rb D_1 line have been observable already at $B \sim 50$ G, but for complete separation one needs to increase a field strength to $B \sim 200$ G (obviously usage of a laser-diode with 1 MHz linewidth would somewhat improve the spectral resolution).

Vertical bars presented on the figures 2 – 4 indicate the frequency position and the magnitude for individual transitions between the Zeeman sublevels obtained by numerical simulations using the model described above. As a result of mixing of the wavefunctions of different hyperfine states, we observe a nonlinear Zeeman effect for a number of sublevels, which results in the following consequences. For the transition ^{85}Rb $F_g = 2$, $m_F = 0 \rightarrow F_e = 3$, $m_F = 0$ (Fig. 3*c*, the 8-th vertical bar from the left) and for the transition ^{85}Rb $F_g = 3$, $m_F = 0 \rightarrow F_e = 2$, $m_F = 0$ (Fig.4*c*, the 3-th vertical bar from the left), the observed frequency shift is of ~ 60 MHz (the case of π excitation). Meanwhile, for a linear Zeeman regime the value of this shift is to be zero (see the diagrams for the case of π excitation in Fig.3*c* and Fig.4*c*, lower part). Another consequence is the substantial modification of transition probabilities between different magnetic sublevels, and appearance of transitions

that are strictly forbidden in the case of a weak magnetic field. As is seen from the figures, a number of new vertical bars with small amplitudes (which are different from the allowed transitions presented on the diagrams of Fig.3, and Fig.4, lower part) already exists at $B \sim 200$ G. Particularly, the peak value of the fluorescence on the transition ^{85}Rb $F_g = 2$, $m_F = 0 \rightarrow F_e = 2$, $m_F = 0$ (Fig.3c) and peak value of the fluorescence on the transition ^{85}Rb $F_g = 3$, $m_F = 0 \rightarrow F_e = 3$, $m_F = 0$ (Fig.4c) has to be zero in the case of a linear Zeeman regime. Meanwhile, in Fig.3c (the 3-rd vertical bar from the left) and in Fig.4c (the 9-th vertical bar mentioned in order of frequency increase) these peaks are distinctly observable as small vertical bars.

In Fig.5a, the results of numerical simulations of frequency position and transition strength are presented for ^{87}Rb D_1 $F_g = 1$, $m_F = -1, 0, +1 \rightarrow F_e = 2$, $m_F = 0, +1, +2$ transitions (σ^+ excitation) and for magnetic field varying in the range of $B = 0 - 1000$ G. A similar plot is presented in the Fig.5b for ^{87}Rb D_1 $F_g = 2$, $m_F = +2, +1, 0 \rightarrow F_e = 1$, $m_F = +1, 0, -1$ transitions (σ^- excitation). Note that the frequency position of the first peak in Fig.5a (transition $F_g = 1$, $m_F = +1 \rightarrow F_e = 2$, $m_F = +2$) has the highest frequency among all Zeeman transitions of Rb D_1 line, and the frequency position of the last peak in Fig.5b, which corresponds to the transition $F_g = 2$, $m_F = +2 \rightarrow F_e = 1$, $m_F = +1$, has the lowest frequency among all Zeeman transitions of Rb D_1 line.

The frequency shift between two side peaks for magnetic field varying in the range of $B = 0 - 1000$ G is presented in Fig.5c (solid line is for $F_g = 1 \rightarrow F_e = 2$, and the dashed line denotes $F_g = 2 \rightarrow F_e = 1$). As it is seen the magnetic field sensitivity of the frequency depends on B, and it lays in the range of $1.6 - 1.9$ MHz/G. The spectral peaks of individual Zeeman transitions are very well pronounced, and a precise measurement of the frequency shift between the two side peaks is possible. This may allow one to design a

simple magnetometer for the B-field range of $50-1000$ G with an unprecedented sub-micron spatial resolution. Although the magnetic field sensitivity of this magnetometer based on ETC (^{87}Rb D_1 $F_g = 1 \rightarrow F_e = 2$ system) will not be as high as the sensitivity of the magnetometers reported in [10, 18], an important advantage could be gained in measuring strong (up to 1000 G) highly inhomogeneous magnetic fields with a strong spatial variation of strength.

It is important to note that in a cell of a usual length ($1 - 10$ cm), there is no evidence of a substructure at $B \sim 200$ G. In order to observe resolved Doppler-broadened transitions between the Zeeman sublevels in the absorption spectrum of a 1 cm-long Rb cell [19], magnetic field $B > 1000$ G was applied. In [20], to observe transitions between the Zeeman sublevels in Cs cell of a usual length placed in a moderate magnetic field $B \sim 250$ G, the non-direct (selective reflection) process has been used.

V. CONCLUSION

It is demonstrated that the use of ETC with the thickness of Rb atomic vapor column $L \approx \lambda/2$ allows one to resolve spectrally large number of individual transitions between Zeeman sublevels of D_1 line of Rb in the sub-Doppler resonant fluorescence excitation spectrum in an external magnetic field of $B \sim 200$ G. The best spectral resolution is achieved for the transitions ^{87}Rb $F_g = 1, 2 \rightarrow F_e = 1, 2$ (all 12 Zeeman components are resolved), and this is caused by "convenient" parameters of the hyperfine levels. In a limited B-field range, a relatively good spectral resolution also could be achieved for ^{85}Rb $F_g = 2 \rightarrow F_e = 2, 3$ (9 resolved components). A partial resolution could be achieved for ^{85}Rb $F_g = 3 \rightarrow F_e = 2, 3$ (from 8 to 10 transitions out of 11 allowed components), whereas in a cell of a usual length ($5 - 50$ mm) there is no structure observed in a spectrum at $B \sim 200$ G.

The spectral resolution of transitions between Zeeman sublevels allows one to easily observe both linear and nonlinear Zeeman effects in the fluorescence spectra obtained with the help of ETC.

The usage of the ETC which is placed in a moderate magnetic field permits to realize "pure" (non-degenerate) atomic transitions system on Rb D_1 line. This technique, which provides a nice demonstration of Zeeman effect by itself, could also be successfully applied for D_1 lines of Cs, K, and other alkali metals.

The proposed ETC-based magnetometer scheme ^{87}Rb D_1 line, which allows for a sub-micron spatial resolution, might be of importance in measuring particular high spatial gradient magnetic fields ($B > 100$ G).

Acknowledgements

The authors are grateful to A. Sarkisyan for his valuable participation in development and fabrication of the ETC. This work was supported, in part, by the Armenian Ministry of Economics – Grants #1351 and #1323.

---

[1] S. Briaudeau, D. Bloch, M. Ducloy. "Detection of slow atoms in laser spectroscopy of a thin vapor film", *Europhys. Lett.* **35**, 337-342 (1996).

[2] S. Briaudeau, D. Bloch, M. Ducloy. "Sub-Doppler spectroscopy in a thin film of resonant vapor", *Phys. Rev. A* **59**, 3723-3735 (1999).

[3] D. Sarkisyan, D. Bloch, A. Papoyan, M. Ducloy. "Sub-Doppler spectroscopy by sub-micron thin Cs-vapor layer", *Opt. Commun.* **200**, 201-208 (2001).

[4] D. Sarkisyan, T. Becker, A. Papoyan, P. Thoumany, H. Walther. "Sub-Doppler fluorescence on atomic D_2 line of sub-micron rubidium vapor layer", *Appl. Phys. B* **76**, 625-631 (2003).

[5] A. Papoyan, D. Sarkisyan, K. Blush, M. Auzinsh, D. Bloch, M. Ducloy. "Magnetic field-induced mixing of hyperfine states of the Cs $6^2P_{3/2}$ level observed with a submicron vapor cell" *Laser Physics* **13**, 1-11 (2003).

[6] D. Sarkisyan, A. Papoyan, T. Varzhapetyan, J. Alnis, K. Blush, M. Auzinsh. "Sub-Doppler spectroscopy of Rb atoms on D_2 line in a sub-micron vapor cell in the presence of a magnetic field". *Journal of Optics A* **6**, S142-S150 (2004).

[7] G. Dutier, A. Yarovitski, S. Saltiel, A. Papoyan, D. Sarkisyan, D. Bloch, M. Ducloy. "Collapse and revival of a Dicke-type coherent narrowing in a sub-micron thick vapor cell transmission spectroscopy". *Europhys. Lett.* **63** (1), 35-41 (2003).

[8] D. Sarkisyan, T. Varzhapetyan, A. Sarkisyan, Yu. Malakyan, A. Papoyan, D. Bloch, M. Ducloy. "Spectroscopy in an extremely thin vapour cell: comparing the cell length dependence in fluorescence and in absorption techniques". Submitted to *Phys. Rev. A*.

[9] D. Sarkisyan, A. Papoyan, T. Varzhapetyan, K. Blush, M. Auzinsh. "Zeeman effect on the hyperfine structure of the D_1 line of a submicron layer of ^{87}Rb vapor". *Opt. Spectrosc.* **96**, 328-334 (2004).

[10] E.B. Aleksandrov, M.P. Chaika, G.I. Khvostenko, *Interference of Atomic States* (Springer-Verlag, New York, 1993).

[11] J.P.Barrat, C.Cohen-Tannoudji, Etude du pompage optique dans le formalisme de la matrice densite, *J. Phys. Rad.* **22**, 329, 443 (1961).

[12] C.Cohen-Tannoudji, *Atoms in strong resonant fields* in Frontiers in Laser Spectroscopy (North-Holland, 1977).

[13] M.P. Auzinsh, R.S. Ferber, Optical-Pumping of Diatomic-Molecules in the Electronic Ground-State - Classical and Quantum Approaches, *Phys. Rev. A* **43**(5), 2374-2386 (1991).

[14] K. Blush, M. Auzinsh, "Validity of Rate Equations for Zeeman Coherences for Analysis of Nonlinear Interactions of Atoms with Laser Radiation", physics/0312124.

[15] M. Auzinsh, R. Ferber, *Optical Polarization of Molecules (*Cambridge University Press, Cambridge, 1995).

[16] R.N. Zare, *Angular Momentum* (J. Wiley and Sons, New York, 1988).

[17] D.A. Varshalovich, A.N. Moskalev, V.K. Khersonskii, *Quantum Theory of Angular Momentum* (World Scientific, Singapore, 1988).

[18] D. Budker, W. Gawlik, D. Kimball, S. Rochester, V. Yaschuk, A. Wies. "Resonant nonlinear magneto-optical effects in atoms". *Rev. Mod. Phys.* **74**, 1153 (2002).

[19] P. Tremblay, A. Michaud, M. Levesque et al. "Absorption profiles of alkali-metal D lines in the presence of a static magnetic field ". *Phys. Rev. A* **42**, 2766-2773 (1990).

[20] N. Papageorgiou, A. Weis, V.A. Sautenkov, D. Bloch, M. Ducloy. "High-resolution selective reflection spectroscopy in intermediate magnetic fields". *Appl. Phys. B* **59**, 123 (1994).

List of Figure Captions

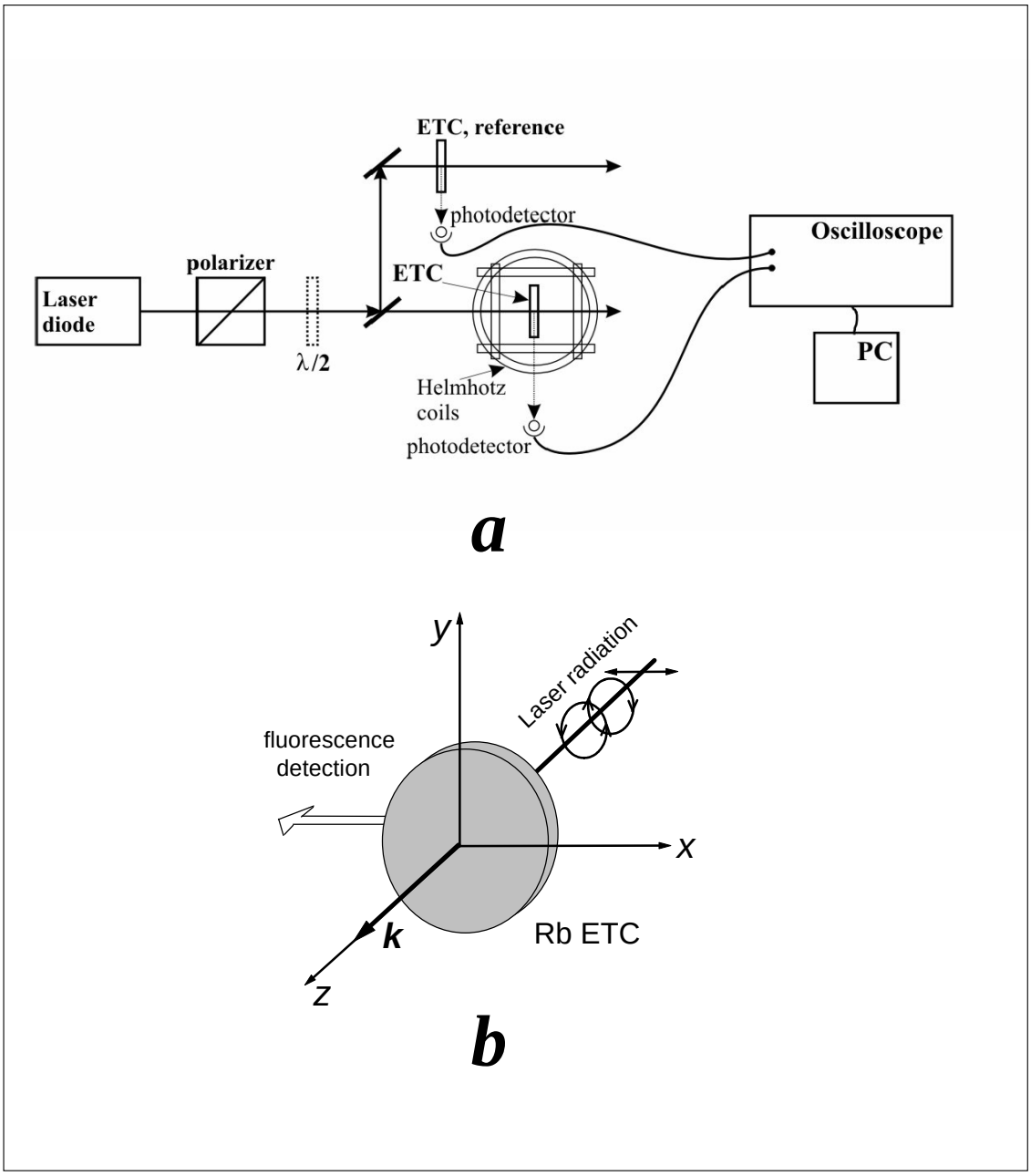

FIG. 1: (a) Schematic diagram of the experimental setup. (b) Geometrical configuration of the experiment. Magnetic field is applied along z or x axes.

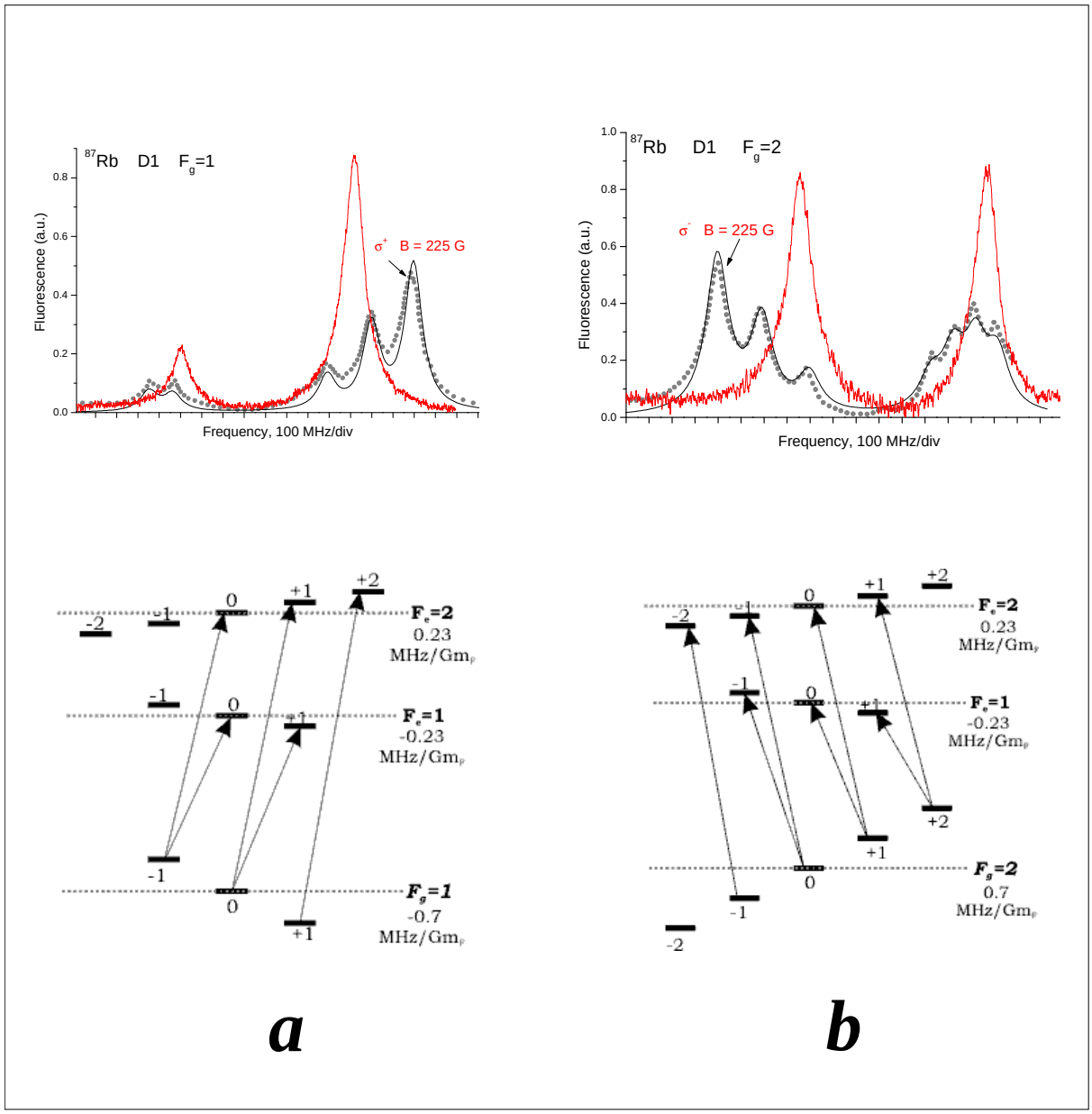

FIG. 2: Resonant fluorescence spectra on D_1 line of ^{87}Rb in an external magnetic filed $B = 225$ G. (a): transitions $F_g = 1 \rightarrow F_e = 1, 2$ with a σ^+ excitation; (b) transitions $F_g = 2 \rightarrow F_e = 1, 2$ with a σ^- excitation. Dots: experiment; solid line – numerical calculations. Light curves here and below show the fluorescence spectra obtained by the second ETC and are used as a frequency and amplitude reference for the case of $B = 0$. On a lower part diagrams of Zeeman sublevels: transitions $F_g = 1 \rightarrow F_e = 1, 2$ (left); transitions $F_g = 2 \rightarrow F_e = 1, 2$ (right) are presented.

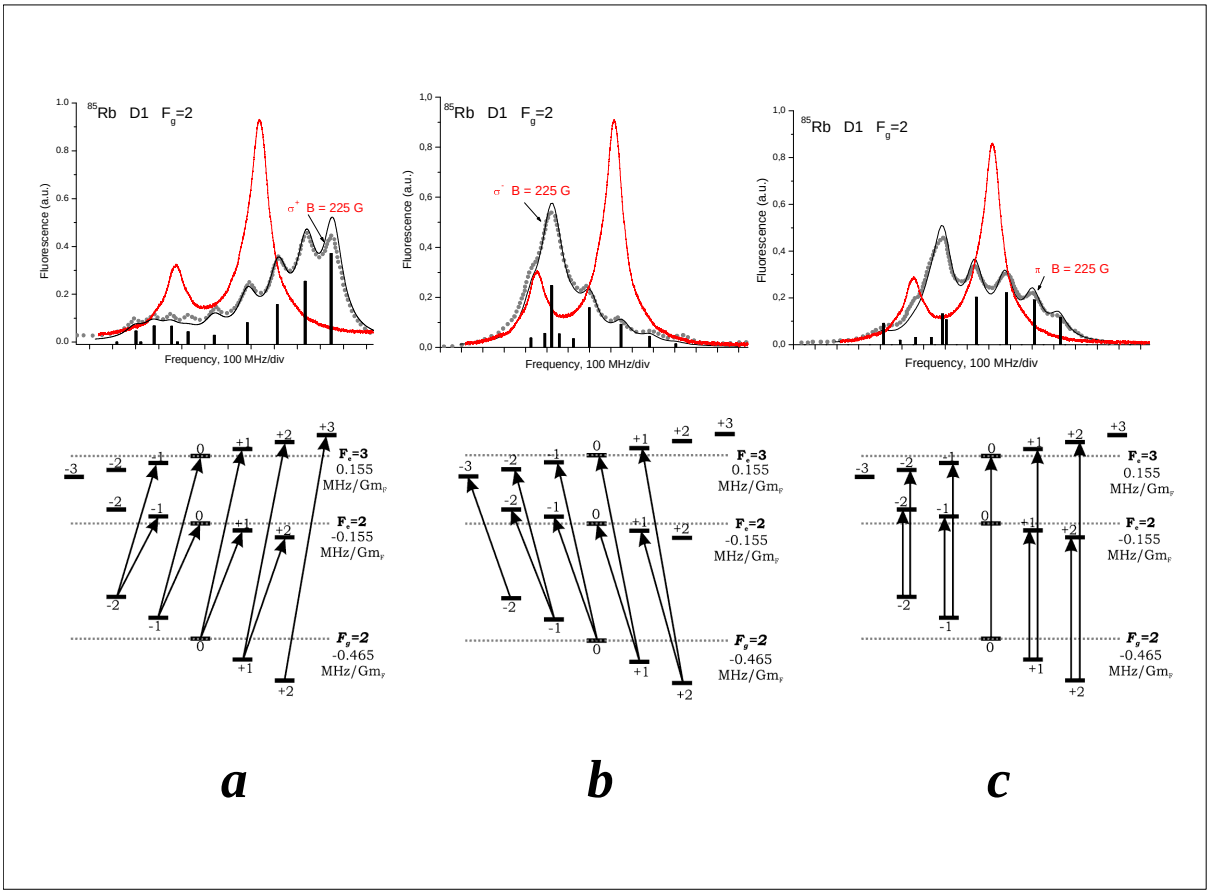

FIG. 3: Resonant fluorescence spectra on D_1 line of ^{85}Rb (transitions $F_g = 2 \rightarrow F_e = 2, 3$) in an external magnetic field 225 G. The excitation polarization: (a) - σ^+, (b) - σ^-, and (c) - π. On a lower part diagrams Zeeman sublevels for σ^+, σ^-, and π excitation correspondingly are presented.

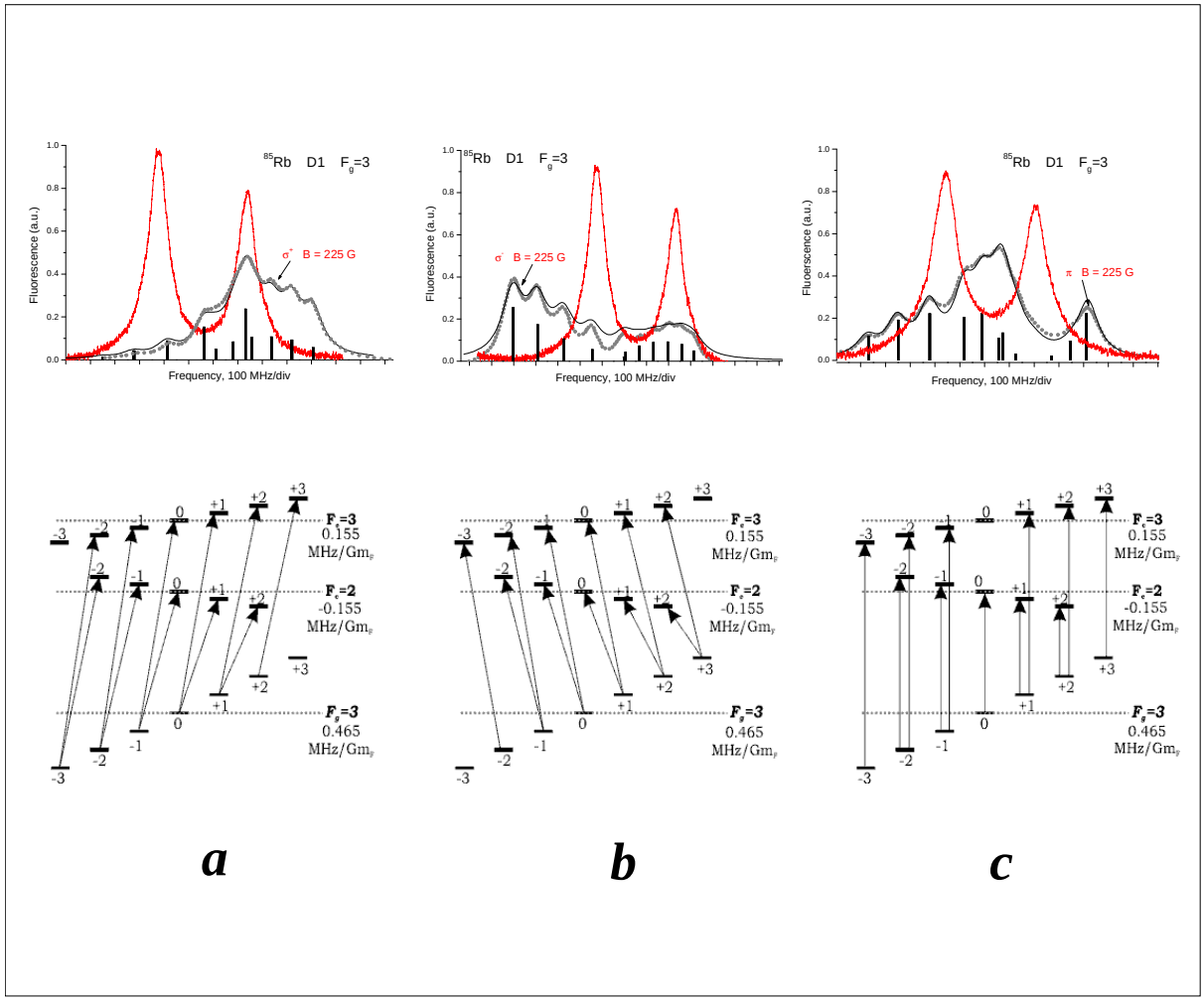

FIG. 4: Resonant fluorescence spectra on D_1 line of ^{85}Rb (transitions $F_g = 3 \rightarrow F_e = 2, 3$) in an external magnetic filed 225 G. The excitation polarization: (a) - σ^+, (b) - σ^-, and (c) - π. On a lower part diagrams of Zeeman sublevels for σ^+, σ^-, and π excitation correspondingly are presented.

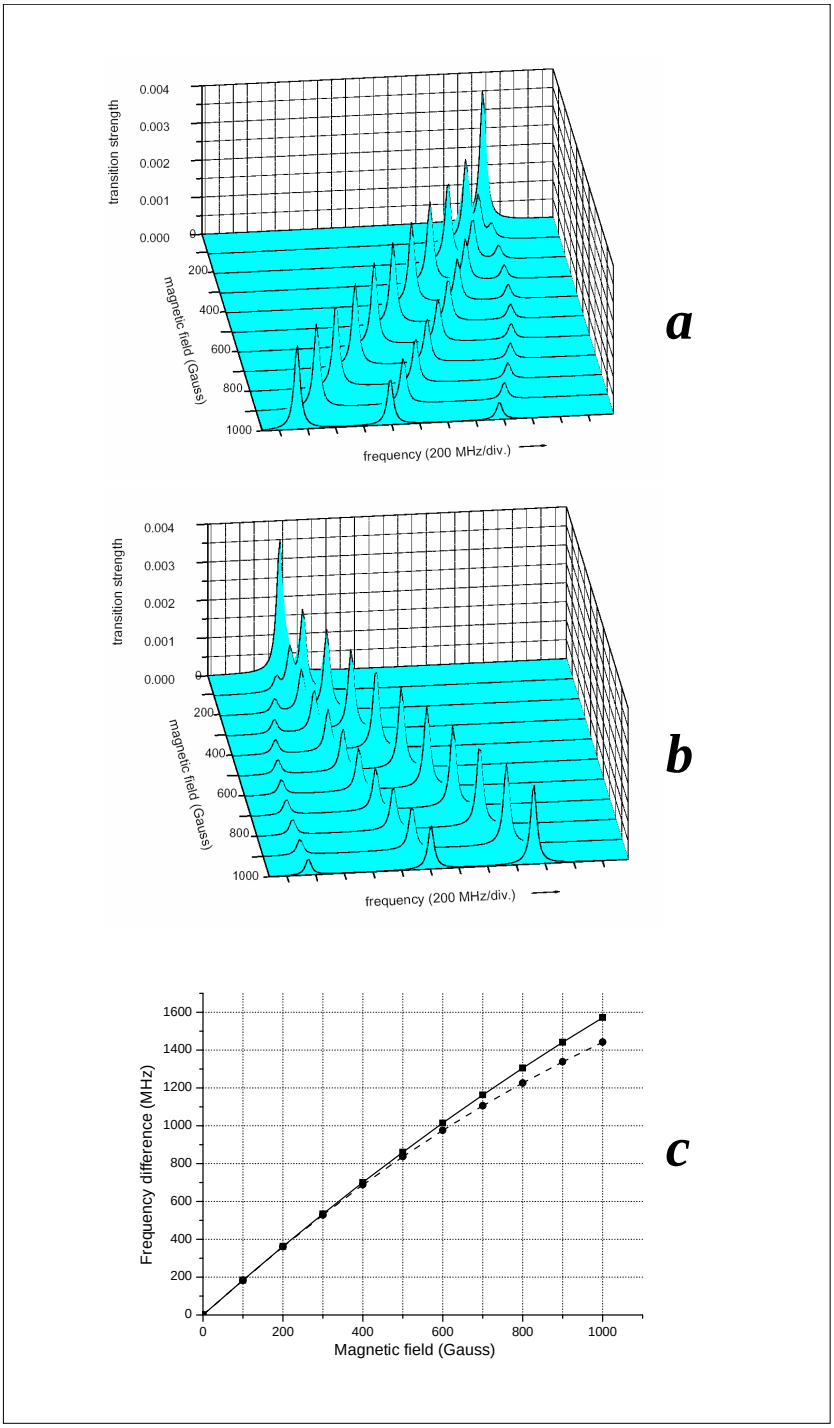

FIG. 5: Dependence of the transition strengths and the transition frequency positions on the magnetic field for: (a) ^{87}Rb D$_1$ $F_g = 1 \rightarrow F_e = 2$ in the case of σ^+ excitation; (b) ^{87}Rb D$_1$ $F_g = 2 \rightarrow F_e = 1$ in the case of σ^- excitation. (c) Magnetic field dependence of the frequency difference between the transitions: $F_g = 1$, $m_F = +1 \rightarrow F_e = 2$, $m_F = +2$ and $F_g = 1$, $m_F = -1 \rightarrow F_e = 2$, $m_F = 0$ (σ^+ excitation, *solid line*); $F_g = 2$, $m_F = 0 \rightarrow F_e = 1$, $m_F = -1$ and $F_g = 2$, $m_F = +2 \rightarrow F_e = 1$, $m_F = +1$ (σ^- excitation, *dashed line*).